Available online at www.sciencedirect.com
SciVerse ScienceDirect
Journal of Genetics and Genomics 39 (2012) 489−502
JGG

METHOD

Development of Novel Visual-Plus Quantitative Analysis Systems for Studying DNA Double-Strand Break Repairs in Zebrafish

Jingang Liu [a,1], Lu Gong [a,1], Changqing Chang [b,1,2], Cong Liu [c], Jinrong Peng [b,*], Jun Chen [a,*]

[a] *College of Life Sciences, Zhejiang University, 866 Yu Hang Tang Road, Hangzhou 310058, China*
[b] *College of Animal Sciences, Zhejiang University, 866 Yu Hang Tang Road, Hangzhou 310058, China*
[c] *Developmental and Stem Cell Institute, West China Second University Hospital, Sichuan University, Chengdu 610041, China*

Received 2 May 2012; revised 26 June 2012; accepted 18 July 2012
Available online 23 August 2012

ABSTRACT

The use of reporter systems to analyze DNA double-strand break (DSB) repairs, based on the enhanced green fluorescent protein (EGFP) and meganuclease such as I-*Sce* I, is usually carried out with cell lines. In this study, we developed three visual-plus quantitative assay systems for homologous recombination (HR), non-homologous end joining (NHEJ) and single-strand annealing (SSA) DSB repair pathways at the organismal level in zebrafish embryos. To initiate DNA DSB repair, we used two I-*Sce* I recognition sites in opposite orientation rather than the usual single site. The NHEJ, HR and SSA repair pathways were separately triggered by the injection of three corresponding I-*Sce* I-cut constructions, and the repair of DNA lesion caused by I-*Sce* I could be tracked by EGFP expression in the embryos. Apart from monitoring the intensity of green fluorescence, the repair frequencies could also be precisely measured by quantitative real-time polymerase chain reaction (qPCR). Analysis of DNA sequences at the DSB sites showed that NHEJ was predominant among these three repair pathways in zebrafish embryos. Furthermore, while HR and SSA reporter systems could be effectively decreased by the knockdown of *rad51* and *rad52*, respectively, NHEJ could only be impaired by the knockdown of *ligaseIV* (*lig4*) when the NHEJ construct was cut by I-*Sce* I *in vivo*. More interestingly, blocking NHEJ with *lig4*-MO increased the frequency of HR, but decreased the frequency of SSA. Our studies demonstrate that the major mechanisms used to repair DNA DSBs are conserved from zebrafish to mammal, and zebrafish provides an excellent model for studying and manipulating DNA DSB repair at the organismal level.

KEYWORDS: DNA DSB repair; NHEJ; HR; SSA; I-*Sce* I; Zebrafish

1. INTRODUCTION

Cells are subjected to a wide range of DNA insults that result from both endogenous and exogenous factors. Endogenous causes of DNA damages include hydrolysis, oxidation, alkylation and errors during DNA replication, while ionizing radiation, ultraviolet radiation, and various chemical agents contribute to some of exogenous DNA damage factors (Hakem, 2008; Ciccia and Elledge, 2010). One of the most genotoxic insults to eukaryotic cells is DNA double-strand break (DSB). If a DNA DSB is not properly repaired, it will result in genomic instability, predisposing the organism to immunodeficiency, neurological disorders and cancer (Thoms

Abbreviations: DSB, double-strand break; EGFP, enhanced green fluorescent protein; HR, homologous recombination; NHEJ, non-homologous end joining; SSA, single-strand annealing; qPCR, quantitative real-time polymerase chain reaction; Lig4, ligaseIV; WT, wild type; CMV, cytomegalovirus; SV40, simian virus 40; hpf, hours post-fertilization.

* Corresponding authors. Tel/fax: +86 571 8898 2101.
E-mail addresses: pengjr@zju.edu.cn (J. Peng); chenjun2009@zju.edu.cn (J. Chen).

[1] These authors contributed equally to this work.

[2] Present address: College of Natural Resources and Environment, South China Agricultural University, Guangzhou 510650, China.

1673-8527/$ - see front matter Copyright © 2012, Institute of Genetics and Developmental Biology, Chinese Academy of Sciences, and Genetics Society of China. Published by Elsevier Limited and Science Press. All rights reserved.
http://dx.doi.org/10.1016/j.jgg.2012.07.009

et al., 2007). To minimize this damage, three efficient DNA DSB repair pathways have been developed to eliminate DSBs and thereafter prevent devastating insults to cells: homologous recombination (HR), non-homologous end joining (NHEJ) and single-strand annealing (SSA). HR ensures high fidelity DNA repair by using the undamaged sister chromatid or homologous DNA as a template to faithfully repair the damage, and is most active in the S and G2 phases of the cell cycle. Apart from the highly conserved recombinase Rad51 which is assumed to be critical for this process, proteins involved in HR also include Rad50, Rad54, RPA, XRCC2, BRCA1, BRCA2, etc (Hiom, 2010). In contrast, NHEJ and SSA are error-prone processes, which are most active during G1 and early S phases. NHEJ facilitates direct rejoining of the two broken ends of the damaged DNA in a sequence-independent manner. Efficient NHEJ requires Ku70/Ku80 heterodimers, DNA-PK catalytic subunit (PKcs), DNA Lig4 and XRCC4 (Weterings and Chen, 2008). SSA is initiated when a DNA DSB occurs between two repeated sequences or within one of two repeated sequences that are in the same direction. Single-stranded DNA is produced at the break point, and this extends to the repeated sequences until the complementary strands can anneal to each other. This annealed intermediate is finally processed by digesting away the single-stranded tails and filling in the gaps. Rad52, Rad59 and RPA are required for the SSA repair pathway (Dudas and Chovanec, 2004).

To investigate these three pathways independently, reporter systems based on the enhanced green fluorescent protein (EGFP) and the I-*Sce* I meganuclease are generally applied. For HR and SSA assays, one 18-bp I-*Sce* I site (Colleaux et al., 1988; Jasin, 1996) was inserted into one copy of a mutant *EGFP* gene, which cannot produce wild-type (WT) EGFP protein. Upon cleavage, the mutant *EGFP* gene could be repaired by either HR with a linked donor *EGFP* gene fragment or SSA with a different design, restoring functional EGFP expression (Pierce et al., 1999; Akyuz et al., 2002; Keimling and Wiesmuller, 2009; Certo et al., 2011). For NHEJ assay, one I-*Sce* I site is inserted between a promoter and the *EGFP* gene to create a DNA DSB, inactivating EGFP protein expression. The DSB created by I-*Sce* I digestion initiates NHEJ, which leads to *EGFP* gene expression. Almost all of these assays were carried out in cell lines. Studies from cell lines showed that the frequencies of HR, SSA and NHEJ varied in different cell types. NHEJ predominates in somatic cells (Lieber et al., 2003; Weinstock et al., 2006) while murine embryonic stem cells utilize HR rather than NHEJ as the principle mechanism of repair (Tichy and Stambrook, 2008; Tichy et al., 2010). However, the roles and the regulation of the three DSB repair pathways during development at the organismal level are unclear. Zebrafish, *Denio rerio*, is an excellent vertebrate model for studying embryogenesis. External development and optical clarity during embryogenesis are especially suitable for visual analysis of DNA DSB repair.

In this study, we carried out DNA DSB repair analysis with zebrafish embryos. By combining EGFP and I-*Sce* I, three constructs were generated for HR, NHEJ and SSA assays, respectively. We used two I-*Sce* I recognition sites in opposite orientation to create DNA DSBs instead of single site used in other I-*Sce* I systems. Results from both the intensities of green fluorescence in the zebrafish embryos and quantitative real-time polymerase chain reaction (qPCR), showed that the use of two opposite I-*Sce* I sites significantly increased the frequencies of HR and SSA, compared to one I-*Sce* I site. Furthermore, interrupting *rad51*, *rad52* and *ligaseIV* (*lig4*) functions impaired repair frequencies of HR, SSA and NHEJ, respectively. Thus, the zebrafish proves to be an ideal model for the study of DNA DSB repair pathways at the organismal level.

2. MATERIALS AND METHODS

2.1. Zebrafish husbandry

Zebrafish wild type (WT) AB strain was used in this study. The animals were raised and maintained at 28.5°C.

2.2. Plasmids construction

2.2.1. HR construction

The pCS2+ vector was used as the backbone. The mutant *EGFP* was amplified by two rounds of PCR. The first round involved two reactions. One reaction amplified the 5′-part of the mutant *EGFP* with forward primer EGFP-5′-F-*Bam*H I and reverse primer mutant EGFP-198-R containing two opposite I-*Sce* I sites. The other reaction amplified the 3′-part of the mutant *EGFP* with forward primer mutant EGFP-202-F harboring two opposite I-*Sce* I sites, and reverse primer EGFP-3′-R. The second round of PCR amplified the full-length mutant *EGFP*, using the two DNA fragments generated in the first round of PCR as templates with two primers: EGFP-5′-F-*Bam*H I and EGFP-3′-R. The full-length mutant *EGFP* was ligated between the Cytomegalovirus (CMV) promoter and the Simian virus 40 (SV40) polyA site in pCS2+. A 5′-EGFP$^{1\text{-}444}$ fragment (encoding the N-terminal 148 amino acids) was then amplified with EGFP-5′-F-*Not* I and EGFP-444-R-*Apa* I and inserted behind SV40 polyA in the recombinant vector.

2.2.2. SSA construction

For the SSA construct, EGFP-5′-F-*Bam*H I and EGFP-444-R-*Xho* I were used to amplify 5′-EGFP$^{1\text{-}444}$ and the resulted fragment was inserted between CMV promoter and SV40 polyA. A second copy of the *EGFP* was amplified from the HR construct with EGFP-5′-F-*Not* I and polyA-*Apa* I-R primers, and cloned into the newly generated vector after the SV40 polyA site.

2.2.3. NHEJ construction

The wild type (WT) *EGFP* was amplified with I-*Sce* I-EGFP-*Bam*H I-F and EGFP-3′-R and cloned into pCS2+.

Primer sequences (5′→3′) for constructing the above plasmids are as follows:

EGFP-*Bam*H I-F: TTACggatccATGGTGAGCAAGGGCGA;

Mutant EGFP-198-R: actgcacgccATTACCCTGTTATCCC TAcgcCATggcatcggTAGGGATAACAGGGTAATgtcatggtggtc acgag;

Mutant EGFP-202-F: accatgacATTACCCTGTTATCCCTA ccgatgccATGgcgTAGGGATAACAGGGTAATggcgtgcagtgctt cag;

EGFP-3′-R:TCAGTctcgagTTACTTGTACAGCTCGTCCAT;

EGFP-444-R-*Apa* I: TCAGTGGGCCCGCTGTTGTAGTT GTACTCCAG;

EGFP-444-R-*Xho* I: TCAGTctcgagGCTGTTGTAGTTGT ACTCCAG;

EGFP-5′-F-*Not* I: TTACgcggccgcATGGTGAGCAAGGG CGA;

PolyA-*Apa* I-R: TCAGTGGGCCCTTAAAAAACCTCCC ACACCTCC;

I-*Sce* I-EGFP-*Bam*H I-F: TTACggatccATTACCCTGTT ATCCCTAccgatgccATGgcgTAGGGATAACAGGGTAATCCC GGGTACCGGTCGCCACCATGGTGAGCAAGGGCGA.

HR, SSA, and NHEJ plasmids were digested with I-*Sce* I meganuclease (New England Biolabs, USA) *in vitro* and then purified with DNA purification kit (Axygen, USA). Cut or uncut HR (100 pg), digested or undigested SSA (25 pg), and digested or undigested NHEJ plasmid (15 pg) were injected into one zebrafish embryo at single-cell stage. The fluorescence was observed through a Nikon AZ100 Fluorescence microscope.

2.2.4. *rad52:EGFP* and *lig4:EGFP* construction

rad52:EGFP or *lig4:EGFP* fragment was amplified from pEGFP vector with a pair of primers: rad52-UTR-EGFP-*Bam*H I-F and EGFP-*Xba* I-R, or a pair of primers: lig4-UTR-EGFP-*Bam*H I-F and EGFP-*Xba* I-R, respectively. DNA fragments were cloned into the pCS2+ vector between CMV promoter and SV40 polyA site, and 15 pg of *rad52:EGFP*, *lig4:EGFP* or pEGFP plasmid was injected into one-cell stage embryo.

Primer sequences (5′→3′) for constructing the above plasmids are as follows:

rad52-UTR-EGFP-*Bam*H I-F: GGATCCACATGGATTAT AGCAGCGGGAGGCAGGTGAGCAAGGGCGAGGAGCTG;

lig4-UTR-EGFP-*Bam*H I-F: GGATCCACAGTTTCTTCC GTGTCTTCTGCAATTATGGTGAGCAAGGGCGAGG;

EGFP-*Xba* I-R: CGCGGATCCATGGTGAGCAAGGGCG AGGAGCTG.

2.3. qPCR and DNA sequencing analysis

In quantitative assays, each experiment for different injections was repeated three times. The numbers of embryos in each injection were from 70 to 150. DNA was extracted from zebrafish embryos with a DNA extraction kit according to the manufacturer's protocol (AidLab #DN08, China). The amount of injected DNA was normalized by normalizing primers with a Bio-rad CFX96/C1000 Real-time PCR machine. Frequencies of HR and SSA repairs were quantified using their respective pairs of repair primers. Frequency of NHEJ repairs was measured using a pair of NHEJ repair primers. To quantify the high-fidelity NHEJ, a second NHEJ repair forward primers (NHEJ repair forward primer-2) was used. The NHEJ repair forward primer-2 was designed from −349 to −334 of the NHEJ construct. The NHEJ repair reverse primer-2 was designed from the DNA sequence of high-fidelity NHEJ at the repaired site. The length of the amplified fragment was 316 bp.

Primer sequences (5′→3′) are as follows:

Normalizing forward primer (Norm-F): ATCATGGCCGA CAAGCAGAAGAACG;

Normalizing reverse primer (Norm-R): CGGCGGCGGT CACGAACTCC;

HR and SSA repair forward primer (HR and SSA-Rep-F): TGACCACCCTGACctacG;

Repair reverse primer (Rep-R): CACCTTGATGCCGTTC TTCTGC;

NHEJ repair forward primer (NHEJ-Rep-F-1): TCGGAG CAAGCTTGATTTAGGTGA;

NHEJ repair forward primer-2 (NHEJ-Rep-F-2): TTGGA AGGACGCCAGG;

NHEJ repair reverse primer-2 (NHEJ-Rep-R-2): CCCGGG ATTACCCTGTTATAACA.

For DNA sequencing analysis, full-length *EGFP* (1−720) was amplified with a pair of primers, using DNA extracted from injected embryos as template. The DNA fragment was cloned to pCS2+ vector and transformed into DH5α cells. Ninety-five clones from the HR assay and 63 clones from the SSA assay were randomly selected for DNA sequencing.

2.4. Morpholinos

Morpholinos were purchased from Gene Tools (USA). *rad51* morpholino (*rad51*-MO) (5′- GGCCATATTTACTCCC GCTAAGCTA-3′), *rad52* morpholino (*rad52*-MO) (5′-TGCCT CCCGCTGCTATAATCCATGT-3′), and *lig4* morpholino (*lig4*-MO) (5′-TTGCAGAAGACACGGAAGAAACTGT-3′) were designed to specifically target the 5′-ATG regions of *rad51* and *rad52*, and 5′-UTR of *lig4*, respectively. The human *β-globin* antisense morpholino (5′-CCTCTTACCTCAGTTA CAATTTATA-3′) was used as standard control (Std-MO). One nanoliter of 1 mmol/L *rad51*-MO, *rad52*-MO and *lig4*-MO was injected into embryos at single-cell stage.

2.5. Protein analysis

For Western blot, total protein was extracted using a standard SDS sample buffer. Western blot was performed as described previously (Chen et al., 2009). Anti-zebrafish Rad51 antibody (AnaSpec #55838, USA) was used to detect Rad51. The anti-EGFP antibody was purchased from Santa Cruz (#SC-9996, USA). After Western blot, the total protein was stained with Coomassie blue and used as the protein loading control.

3. RESULTS

3.1. Reporter assay systems for HR, SSA and NHEJ DNA DSB repairs in zebrafish embryos

To set up the reporter systems for DNA DSB repair analysis in zebrafish, we first followed the designs of the assay constructs established in cell lines (Keimling and Wiesmuller,

2009). One I-*Sce* I site was inserted into the *EGFP* coding sequence to generate a mutant *EGFP*. However, with such a system employed in zebrafish, green fluorescence was hardly detectable in the HR assay and only weak signal was observed in the SSA assay (data not shown). It is known that DSB with flushed 5′-phosphorylated ends or complementary overhangs can be re-ligated efficiently by NHEJ (Wilson et al., 1982). We reasoned that the low HR repair frequency in this situation may be due to the complementary overhangs, with 5′-phosphorylated ends generated by the endonuclease I-*Sce* I digestion at one site *in vitro*, resulting in most of the DSB repairs through direct end re-ligation. To overcome this preferred repair mechanism of straight ligation which largely diminishes the routes of HR and SSA, we modified the design by using two I-*Sce* I sites in opposite orientation instead of the usual single site to generate mutant *EGFP* (Fig. 1A). The recognition site of I-*Sce* I (18 bp) is not a palindromic sequence. Both of the forward and reverse I-*Sce* I sites produce -TTAT-3′ overhangs after I-*Sce* I digestion, which partially complement each other. In addition, to ensure that the mutant *EGFP* would not produce wild type green fluorescent protein, a 14 bp DNA sequence flanked with two I-*Sce* I sites in the opposite direction was used to substitute 4 bp (from 198 to 201) of *EGFP* in the *EGFP* chromophore-encoding region. Thus the structure of *EGFP* chromophore would be damaged and the coding sequence of *EGFP* from 202 to 720 (3′ end) was not in frame with the first ATG of *EGFP* in mutant *EGFP*. To record HR exclusively, only the coding sequence from 1 to 444 of 5′-$EGFP^{1\text{-}444}$ was used as the donor template. The HR construct will not express the WT EGFP protein if SSA repair occurs after the initiation of DSB repair, since SSA repair will only result in a copy of 5′-$EGFP^{1\text{-}444}$ without the SV40 terminator. SSA construct was generated as described in Fig. 1A. When the SSA repair was initiated, the intermediate DNA sequence between 5′-$EGFP^{1\text{-}444}$ and the mutant *EGFP* was digested to form a WT *EGFP*. The SSA construct will not express WT EGFP if it is repaired by HR. Although HR can use 5′-$EGFP^{1\text{-}444}$ as a template to repair the mutant *EGFP*, the repaired *EGFP* fails to be expressed devoid of a promoter. To ensure that uncut NHEJ construct would not express EGFP, we introduced a start codon (ATG) into 14 bp between the two I-*Sce* I sites, which is not in frame with the coding sequence of *EGFP*.

The three constructs were digested with I-*Sce* I *in vitro*. Both I-*Sce* I-cut and uncut plasmids were injected separately into zebrafish embryos. Green fluorescence was observed under a fluorescence microscope at 4, 7 and 10 hours post-fertilization (hpf). As expected, no green fluorescence was detected in the embryos injected with uncut constructs (Fig. 1B). Meanwhile, EGFP could be observed in the embryos injected with the three cut constructs at 7 hpf with gradually increased over time (Fig. 1B). Although the green fluorescence was weak, moderate and strong in the HR, SSA, and NHEJ repair (Fig. 1B), respectively, our observations suggested that the three DNA DSB repair pathways HR, SSA and NHEJ were successfully initiated in zebrafish embryos using the modified design with two opposite I-*Sce* I sites.

3.2. Quantitative assay to determine the frequencies of HR, SSA and NHEJ with qPCR

In previous cell line assay systems, the frequencies of the three DNA DSB repair mechanisms are quantitatively measured by fluorescence activated cell sorting (FACS) analysis as the fraction of green fluorescing cells within the transfected cell population. However, FACS analysis at organism level is not as straight forward as cell line systems and it can only distinguish EGFP positive and negative cells, but cannot measure the absolute EGFP intensity of each cell. Thus, considering that the number of plasmids entering each cell varies in the transient transfection or injection systems, we reckoned that FACS analysis would not provide an accurate measurement and therefore is not the best way for direct comparison of the repair efficiencies of HR, SSA and NHEJ in a transient transfection or injection assays. We therefore developed a method to quantitatively analyze the frequencies of the three DNA DSB repairs using qPCR. Three pairs of primers were designed (Fig. 2A). The first were the normalized primers and they amplified a 229 bp DNA fragment from 457 to 685 of *EGFP* (Fig. 2A). As this fragment would be intact in both of the cut and uncut plasmids of the three constructs, these primers were used to normalize the total amount of injected plasmids. The second pair of primers were the HR and SSA repair primers and they amplified a 307 bp DNA fragment from 185 to 492 of WT *EGFP* (Fig. 2A). It was expected that the second pair of primers could only anneal with the templates from WT *EGFP* or the correctly repaired mutant *EGFP* either by HR or by SSA, and could not anneal with the cut, uncut or incorrectly repaired mutant EGFPs. In another word, they could not amplify the fragment from either 5′-$EGFP^{1\text{-}444}$ or the mutant *EGFP*. The third pair of primers were the NHEJ repair primers and they amplified a 626 bp DNA fragment from −133 to 492 of *EGFP* (Fig. 2A). As two I-*Sce* I sites were inserted within the amplified fragment, the third pair of primers could only use the uncut NHEJ construct as a template.

As expected except the negative control (Fig. 2B), a 229 bp normalized DNA fragment was amplified from all of the templates including a WT *EGFP* plasmid (positive control), the uncut and cut HR plasmids, the uncut and cut SSA plasmids, and the uncut and cut NHEJ plasmids (Fig. 2B). Meanwhile, the HR and SSA repair fragment was amplified only from the WT *EGFP* plasmid, but not from the uncut and cut HR plasmids, the uncut and cut SSA plasmids; the NHEJ repair fragment was amplified from the uncut NHEJ plasmid, but not from the cut NHEJ plasmid (Fig. 2B).

To test whether these three pairs of primers could be used to analyze DNA repair frequencies of the assay constructs repaired *in vivo*, the I-*Sce* I-cut and uncut plasmids were injected into fertilized zebrafish eggs. The results of green fluorescence observation were similar to those in Fig. 1B. Then, DNA was extracted from the injected embryos at 10 hpf. Normalizing fragment was amplified from all of the DNA samples except those extracted from uninjected embryos (negative control) (Fig. 2B). The HR and SSA repair fragment

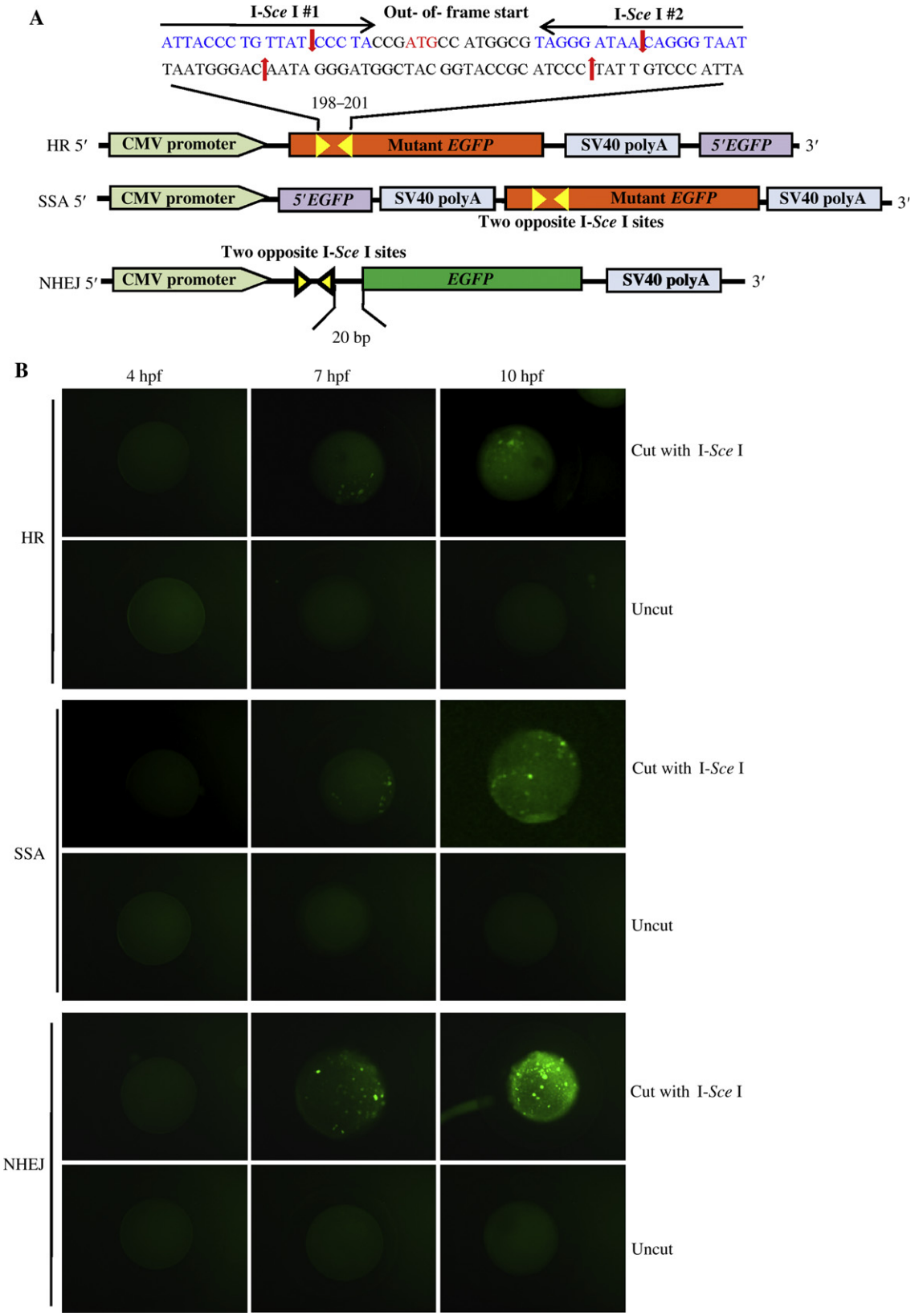

Fig. 1. Reporter assay systems for HR, SSA, and NHEJ DNA DSB repairs in zebrafish embryos.

A: diagram of HR, SSA and NHEJ. The two opposite I-*Sce* I recognition sequences are in blue; the interspace sequence between two I-*Sce* I sequences are in black; introduction of the new start codon ATG is in red; red arrows indicate the cut sites of I-*Sce* I; HR: the mutant *EGFP* is expressed by the CMV promoter and terminated by SV40 polyA; the yellow triangle indicates the I-*Sce* I recognition site; 198−201 is the 4 bp sequence of WT *EGFP*; SSA: 5′-*EGFP* is driven by the CMV promoter and terminated by SV40 polyA; the mutant *EGFP* has no promoter; NHEJ: the distance between the two opposite I-*Sce* I sites and the start codon of *EGFP* in NHEJ is 20 bp. **B:** the observation of fluorescence for HR, SSA and NHEJ in zebrafish embryos.

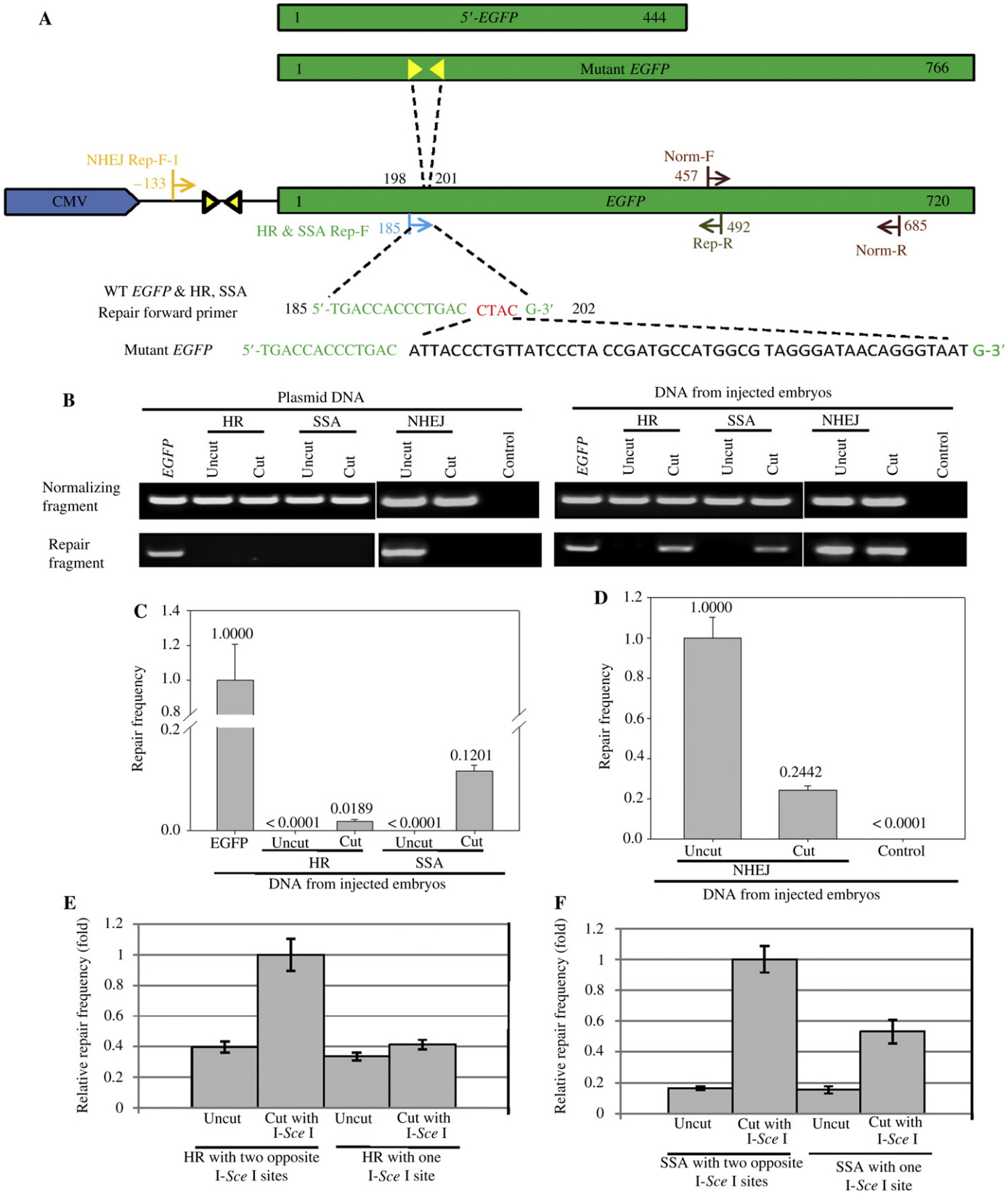

Fig. 2. Quantitative assay for the frequencies of HR, SSA and NHEJ with qPCR.

A: diagram of three pairs of primers for qPCR. The normalizing primers of *EGFP* are in brown: forward primer from 457−481, reverse primer from 666−685; HR and SSA repair primers: the forward primer from 185−202 of WT *EGFP* is in green, which covers the mutation site in the mutant *EGFP* such as the substitution of 4 bp (198−201) of the WT *EGFP* sequence in red with 50 bp DNA (two I-*Sce* I sites) in black, and the reverse primer from 471−492 in dark green; NHEJ repair primers: the forward primer from −133 to −110 is in orange, the reverse primer is the same as the HR and SSA repair reverse primer. **B:** PCR analysis of the three

was amplified from samples injected with the WT *EGFP* (positive control), cut HR and SSA, but not from samples injected with uncut HR or SSA (Fig. 2B). The NHEJ repair fragment was amplified from samples injected either with the uncut or cut NHEJ, but not from negative control (Fig. 2B). Next, we measured the frequencies of HR, SSA and NHEJ repairs *in vivo* by qPCR. Our results showed that the frequencies of HR and SSA were 1.89% and 12.01%, respectively, when the embryos injected with WT *EGFP* were used as the control for accurate repair (Fig. 2C); and the frequency of NHEJ was 24.42% when the embryos injected with uncut NHEJ was used as the repair control (Fig. 2D). In addition, we also used qPCR to compare the frequencies of HR and SSA initiated by DNA DSB created with either one I-*Sce* I or two opposite I-*Sce* I sites. Our results showed that the addition of an extra I-*Sce* I site in opposite orientation produced a 2.5- and 1.8-fold increase in HR (Fig. 2E) and in SSA (Fig. 2F), respectively, consistent with the intensity of green fluorescence observed in each reporter system (data not shown).

3.3. NHEJ is predominant among the three DNA DSB repair pathways during early embryogenesis

To further characterize the choice between different DSB repair pathways in zebrafish embryos, we carried out DNA sequence analysis at the DSB site. DNA was extracted from embryos injected with either the cut HR or SSA. A pair of primers were designed to amplify the entire mutant *EGFP* sequence. PCR fragments were ligated to a vector and recombinant plasmids were transformed into *Escherichia coli* cells. Plasmids DNA extracted from randomly picked colonies were subjected to DNA sequencing. A total of 95 clones from the HR assay and 63 clones from the SSA assay were sequenced (Tables 1 and 2). DNA sequencing showed that none of the 158 clones yielded a complete sequence of mutant *EGFP* clones, suggesting that the digestion with I-*Sce* I was relatively complete *in vitro*. In the HR report system, about 20% (19/95) of the repaired DSBs were identical to WT *EGFP* (Table 1). The sequencing results also revealed that the remaining about 80% of the repaired DSBs in the HR assay were carried out *via* the NHEJ pathway (Table 1). In the SSA reporter system, about 24% (15/63) of the repaired DSBs were carried out *via* the SSA pathway with the remaining 76% *via* NHEJ (Table 2). Our data imply that there was a competition, either between HR and NHEJ in the HR assay, or between SSA and NHEJ in the SSA assay. Nevertheless, NHEJ is found to be predominant in zebrafish embryos, similar to the previous discoveries (Hagmann et al., 1998).

The sequencing results also showed that there were two main sub-types of NHEJ. The first was high-fidelity NHEJ (Tables 1 and 2). In general, digestion of the two opposite I-*Sce* I sites generates two partially complementary 3′ overhangs: -TTAT (5′ → 3′) and TATT- (3′ → 5′). If the partially complementary ends annealed without DNA-end resection, a two base gap would occur on both strands which could be filled in by a gap-filling polymerase. This would result in a repaired joint with the sequence -TTATAA-, which is defined as high-fidelity NHEJ (Adams et al., 2010). The second type is non-high-fidelity NHEJ. Sequences from this type of repair contain sequence changes at the break sites, including small deletions of 1−3 nucleotides or larger deletions. Interestingly, the frequency of high-fidelity NHEJ (7/95) from the HR construct (Table 1) was much lower than that from the SSA construct (36/63) (Table 2), suggesting that the HR design decreased the number of high-fidelity NHEJ repairs. Taken together, we have showed that the three reporter systems worked efficiently in zebrafish embryos. Furthermore, NHEJ predominates among the three DNA DSB repair mechanisms in zebrafish embryos.

3.4. Knockdown of *rad51* impaired HR

To test whether these three reporter systems can be used to study gene functions in zebrafish embryos, we started from impairing the function of *rad51*, the critical recombinase for HR in all eukaryotic organisms (Porter et al., 1996; Sung et al., 2003). For this purpose, a *rad51*-MO was designed to block protein translation by targeting its 5′-ATG region (GenBank accession No. BC062849). An antibody that specifically recognizes zebrafish Rad51 was used to analyze the expression of endogenous Rad51 protein. Our results showed that the Rad51 protein level in the embryos injected with *rad51*-MO (Fig. 3A) was considerably lower than that in the embryos injected with the Std-MO, which suggested that the protein translation of *rad51* was successfully blocked by *rad51*-MO (Fig. 3A). To investigate the effect of *rad51*-MO on HR, we injected cut HR and co-injected cut HR with either *rad51*-MO or Std-MO into zebrafish embryos. At 10 hpf, green fluorescence was observed and DNA was extracted and subjected to qPCR assay. An obvious decrease in green fluorescence intensity was found in the embryos co-injected with the cut HR and *rad51*-MO, compared to those co-injected with HR and Std-MO, or the embryos injected with cut HR alone (Fig. 3B). These observations were supported by the results obtained from our qPCR assays where knockdown of *rad51* produced a three-fold reduction in the frequency of HR (Fig. 3C). Meanwhile, *rad51* morphants developed abnormally with most of them underdeveloped with curved bodies at 48 hpf, compared to those embryos co-injected with Std-MO (Fig. S1). These data highly favor the utilization of the zebrafish model system to systemically study gene functions in the HR pathway and its roles in embryonic development.

pairs of primers. Different plasmid DNAs (left panel) and DNAs extracted from the embryos injected with different plasmids, as indicated at 10 hpf, were used as the template to conduct PCR with the three pairs of primers. **C:** frequencies of the HR and SSA repairs analyzed with qPCR. The WT *EGFP* plasmid injection was used as a 100% accurate repair control for the HR and SSA assays. **D:** frequency of NHEJ repair. The uncut NHEJ plasmid injection was used as a 100% repair control. **E** and **F:** quantitative analysis to compare the frequencies of HR (**E**) and SSA (**F**) with two opposite I-*Sce* I sites to the frequencies with one I-*Sce* I site. The three pairs of primers were used to quantify the repair frequencies of DNA DSB repairs from the different samples as indicated.

Table 1
Sequence analysis from HR assay

	Sequence (5′→3′)	Frequency
WT *EGFP*	ACCCTGAC- -CTAC- -GGCGTG	
Mutant *EGFP*	ACCATGACattaccctgttatccctaCCGATGCCatgGCGtagggataacagggtaatGGCGTG	
HR events	ACCCTGAC- -CTAC- -GGCGTG	19/95
Different NHEJ events	ACCATGACATTACCCTGTTAT- - - - - - - - - - - - - - - - -AACAGGGTAATGGCGTG	7/95
	ACCATGACATTACCCTGTT- -AACAGGGTAATGGCGTG	3/95
	ACCATGACATTACCCTGTTAT- - - - - - - - - - - - - - - - - - - -CAGGGTAATGGCGTG	2/95
	With more deletion	64/95

The green nucleotides indicate WT or correctly repaired *EGFP*, and the red nucleotides indicate 3′ overhangs nucleotides after I- *Sce* I digestion.

3.5. The frequency of SSA was significantly reduced by knockdown of *Rad52*

Next, knockdown of *rad52* gene was used to interfere with the SSA repair pathway. The *rad52* gene is reported to be the important factor in mediating SSA process by searching homologous sequence flanking the DSB (Ivanov et al., 1996). To evaluate *rad52* function in zebrafish embryos, we designed a *rad52*-MO to block protein translation by targeting its 5′-UTR region (GenBank accession No. BC098627). To check the potency of the morpholino, the 5′-UTR sequence of *rad52* was cloned upstream of *EGFP* to form *rad52:EGFP*. The *rad52*-MO was co-injected with either *rad52:EGFP* plasmid or *CMV:EGFP* plasmid into zebrafish embryos. At 10 hpf, green fluorescence was observed (Fig. 4A) while total proteins were extracted and subjected to Western blot analysis to check EGFP level (Fig. 4B). As expected, *rad52*-MO efficiently blocked EGFP expression in the embryos co-injected with *rad52:EGFP*, but not those with *CMV:EGFP* (Fig. 4A). Next, to study the influence of *rad52*-MO on SSA, *rad52*-MO was co-injected with cut SSA, using Std-MO as the morpholino co-injection control. Results from both green fluorescence observation (Fig. 4C) and qPCR analysis (Fig. 4D) showed that there was a seven-fold decrease in the frequency of SSA due to the knockdown of *rad52* (Fig. 4D). The morphants co-injected plasmid with *rad52-MO* also developed abnormally at 48 hpf (Fig. S2), but not as severe as those injected with *rad51*-MO (Fig. S1). Our data demonstrate that the loss function of *rad52* not only impairs the SSA pathway but also results in abnormal embryo development in zebrafish.

3.6. NHEJ was only affected by *lig4* knockdown when NHEJ construct was cleaved by I-*Sce* I *in vivo*

Finally, to test the NHEJ reporter construct in zebrafish embryos, we chose *lig4*, which encodes a DNA ligase that directly ligates DNA DSBs and therefore is absolutely required for the NHEJ pathway (Mills et al., 2004). To study *lig4* function on NHEJ in zebrafish embryos, we employed a similar method to that used in the studies of *rad51* and *rad52* above. A *lig4*-MO was designed to block *lig4* translation by targeting its 5′-UTR region (GenBank accession No. NM_001103123). A *lig4:EGFP* plasmid containing 5′-UTR sequence of *lig4* upstream of *EGFP* was generated to check the potency of the morpholino. Results from both fluorescence observation and EGFP protein assay demonstrated that the *lig4*-MO worked efficiently (Fig. 5A and B). However, functional study on NHEJ, from both fluorescent observation and quantitative assay, showed that *lig4*-MO did not interrupt NHEJ (Fig. 5C and D). This might be due to the presence of maternal Lig4 protein. To test this supposition, we tried postponing NHEJ to a later stage, when maternal Lig4 protein ran out and NHEJ required *de novo* synthesized Lig4 protein. We would expect NHEJ to be affected in the later stage if the

Table 2
Sequence analysis from SSA assay

	Sequence (5′→3′)	Frequency
WT *EGFP*	ACCCTGAC- -CTAC- -GGCGTG	
Mutant *EGFP*	ACCATGACattaccctgttatccctaCCGATGCCatgGCGtagggataacagggtaatGGCGTG	
HR events	ACCCTGAC- -CTAC- -GGCGTG	15/63
Different NHEJ events	ACCATGACATTACCCTGTTAT- - - - - - - - - - - - - - - - -AACAGGGTAATGGCGTG	36/63
	ACCATGACATTACCCTGTT- -AACAGGGTAATGGCGTG	5/63
	ACCATGACATTACCCTGTTAT- - - - - - - - - - - - - - - - - - - -CAGGGTAATGGCGTG	3/63
	With more deletion	4/63

The green nucleotides indicate WT or correctly repaired *EGFP*, and the red nucleotides indicate 3′ overhangs nucleotides after I- *Sce* I digestion.

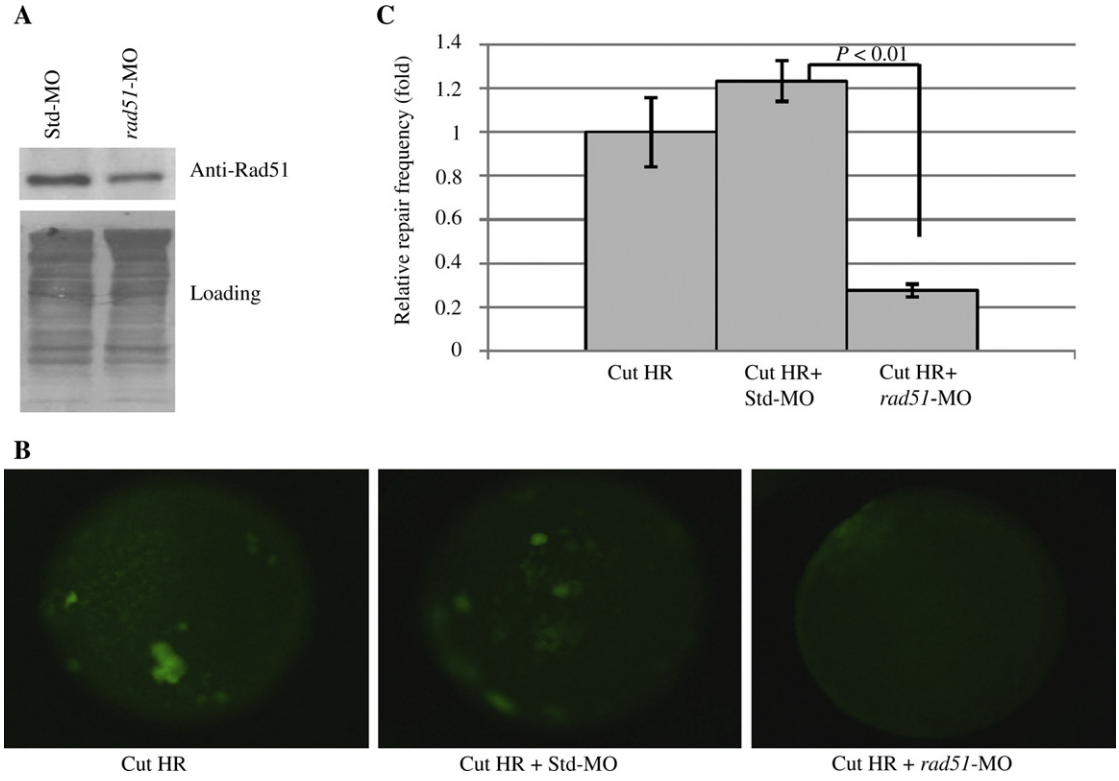

Fig. 3. Knockdown of *rad51* with *rad51*-MO impairs HR.
A: Western blot analysis of Rad51 proteins from different morphants as indicated. Anti-zebrafish Rad51 antibody was used to detect the endogenous Rad51. **B:** fluorescent observation of HR repair from different samples as indicated. **C:** the frequencies of HR repairs analyzed by qPCR.

translation of *de novo* Lig4 protein was blocked. When we used *in vitro* cut plasmid to analyze NHEJ, only 15 pg of the cut NHEJ construct was required to be injected into one embryo. If the amount of the cut plasmid was increased to 20 pg, the fluorescence would be observed as early as 4 hpf (data not shown). To postpone NHEJ, we co-injected 50 pg of the uncut NHEJ plasmid with *I-Sce I* mRNA into each embryo to cut the NHEJ construct *in vivo* to delay DNA repair. As expected, fluorescence was only observed in the co-injected embryos at 14 hpf, but not in the embryos injected with the uncut NHEJ construct alone (Fig. 5E). Next, we co-injected a mixture of *lig4*-MO, NHEJ uncut plasmid and *I-Sce I* mRNA into the embryos, with Std-MO used as morpholino co-injection control. There was a clear decrease in the intensity of green fluorescence in the embryos co-injected with *lig4*-MO, compared to those co-injected without *lig4*-MO (Fig. 5E). Since the NHEJ repair primers can utilize the uncut NHEJ as template (Fig. 2B), a new pair of NHEJ repair primers (NHEJ-Rep-2) were designed, which could only use the DNA repaired by high-fidelity NHEJ as a template, but not the uncut NHEJ. The qPCR analysis (Fig. 5F) showed that knockdown of *lig4* resulted in a three-fold reduction in the number of NHEJ repairs. Meanwhile *lig4*-MO injection brought about severe phenotypes on embryo development with 66% morphants died at 24 hpf and the rest suffered developmental delay (Fig. S3). These data suggest that NHEJ is active during embryonic development at the very early stage.

3.7. Blocking NHEJ with *lig4*-MO increased the frequency of HR, but decreased the frequency of SSA

An inherent competition exists among different DSB repair pathways. Our data above demonstrated that NHEJ is the principal mechanism among the three repair pathways in zebrafish embryos. To test whether blocking NHEJ has an effect on HR and SSA, we co-injected *lig4*-MO either with the cut HR or the cut SSA plasmid, with Std-MO as the morpholino co-injection control. Very interestingly, blocking NHEJ with *lig4*-MO significantly increased the frequency of HR (Fig. 6A and B) but decreased the frequency of SSA (Fig. 6C and D) compared to those co-injected with Std-MO controls. These results suggested that there is a competition between NHEJ and HR repairs. Also, *lig4* is required for SSA repair.

4. DISCUSSION

Most of the existing reporter assays have been carried out in somatic cell culture systems. The studies from cell lines show that NHEJ is predominant in somatic cells (Lieber et al., 2003; Weinstock et al., 2006), and on the contrary, HR is preferred in embryonic stem cells (Tichy and Stambrook, 2008; Tichy et al., 2010). Furthermore, a study on the roles of NHEJ and HR during mice embryonic development reported quite similar results to those in embryonic cells. *Xrcc2* knockout (defective HR) mice showed abundant apoptosis and early

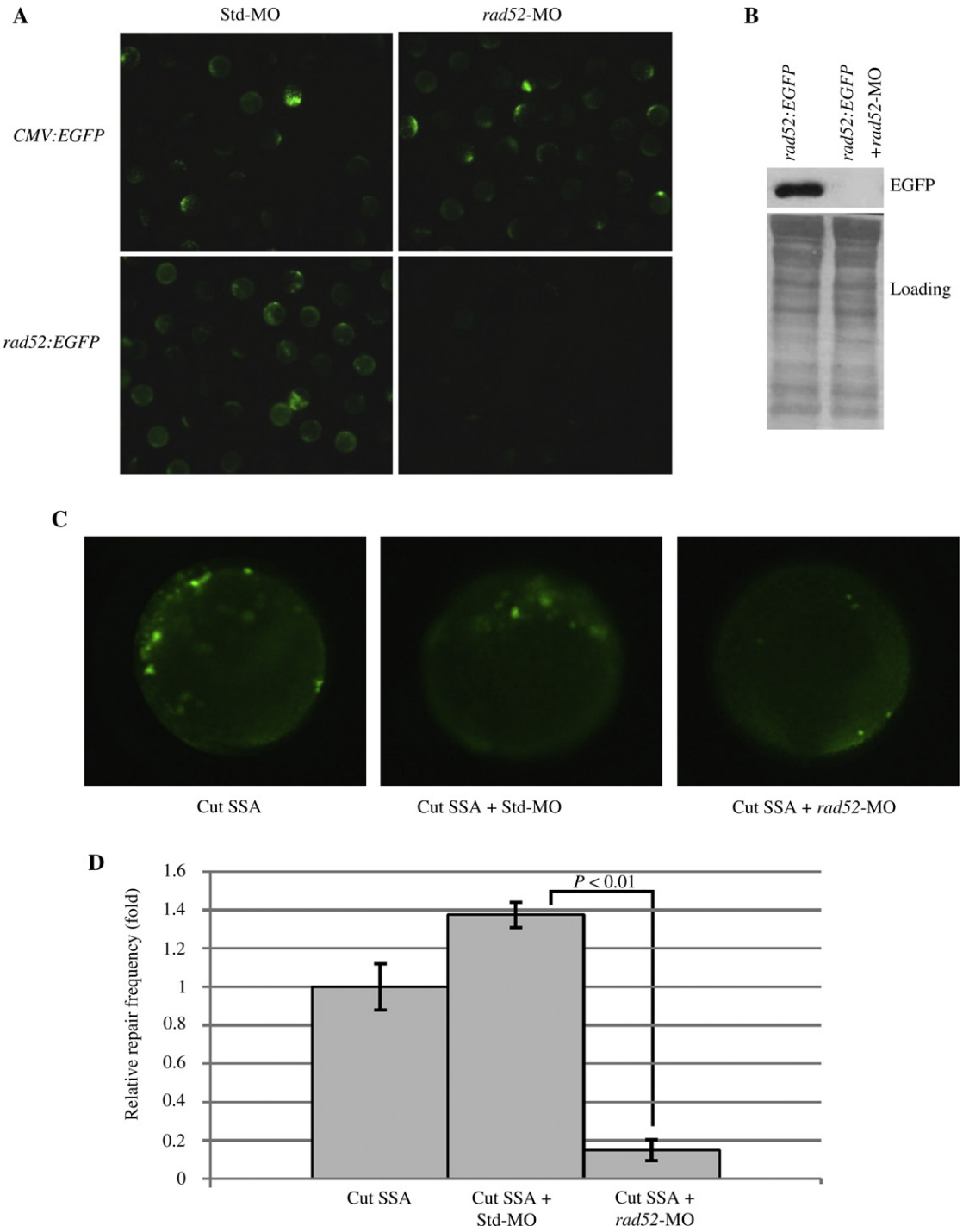

Fig. 4. The frequency of SSA was significantly reduced by knockdown of *rad52*.
A: knockdown Rad52 protein expression with *rad52*-MO. *CMV:EGFP* or *rad52:EGFP* was co-injected either with Std-MO or with *rad52*-MO. **B:** Western blot analysis of EGFP protein in the embryos as indicated using EGFP antibody. **C:** fluorescent observation of SSA repair from different samples as indicated. **D:** the frequencies of SSA repairs analyzed by qPCR.

mortality around embryonic days 9−10 (E9−E10) (Orii et al., 2006). In contrast, disruption of NHEJ resulting from *Lig4* knockout had no obvious phenotypes until E12. These results indicate that NHEJ may be dispensable before mid-gestation, as DSB repair during this period mainly utilizes HR. The studies from either cell lines or knockout mice suggest that distinct repair pathways are differentially activated in different developmental stages or cell types. However, the studies based on the mouse knockout system or embryonic stem cells do not precisely reflect the situation of DSB repair during embryonic

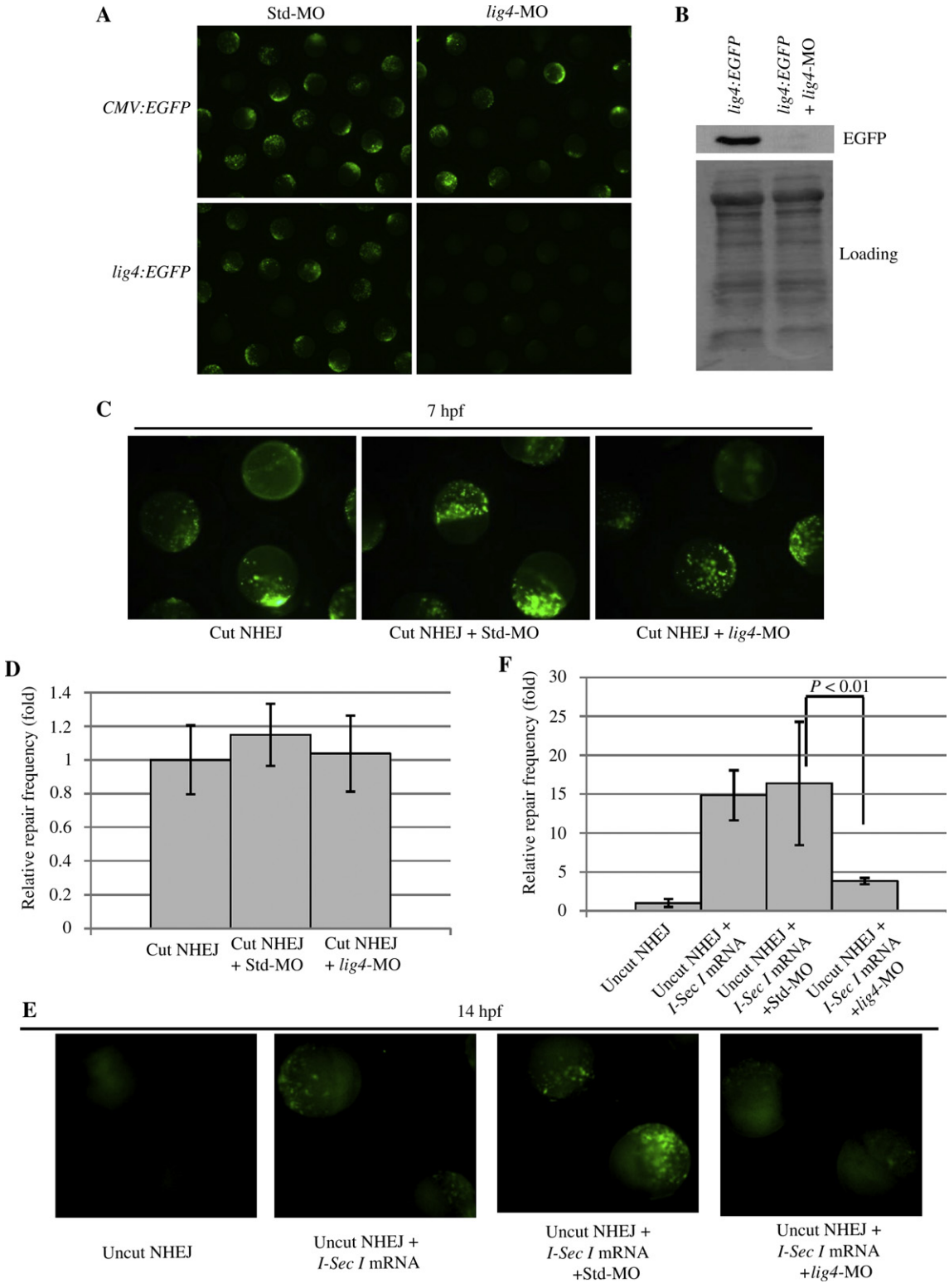

Fig. 5. Influence of *lig4* knockdown by *lig4*-MO on NHEJ.

A: knockdown Lig4 protein expression with *lig4*-MO. *CMV:EGFP* or *lig4:EGFP* was co-injected either with Std-MO or with *lig4*-MO. **B:** Western blot analysis of EGFP protein in the embryos using EGFP antibody. In **C** and **D**, NHEJ plasmid was cut with I-*Sce I in vitro*, then co-injected either with Std-MO or with *lig4*-MO. NHEJ repair analysis was carried out either by fluorescent observation (**C**) or by qPCR using a pair of NHEJ repair primer-2 (**D**). In **E** and **F**, NHEJ plasmid was mixed with *I-Sce I* mRNA and co-injected either with Std-MO or with *lig4*-MO. NHEJ repair analysis was carried out either by fluorescent observation (**E**) or by qPCR (**F**).

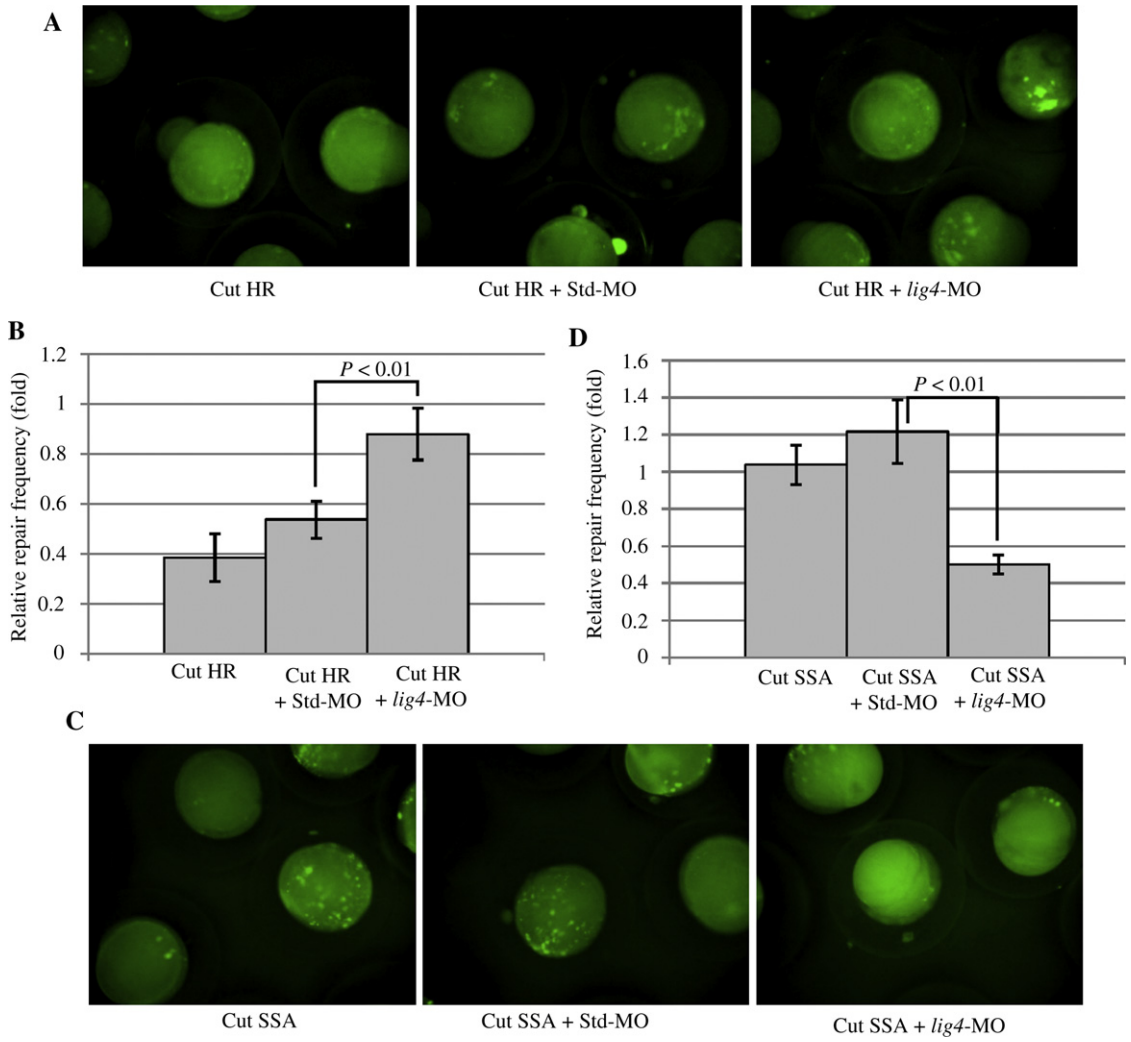

Fig. 6. Influence of *lig4* knockdown by *lig4*-MO on HR and SSA.
A and **B:** HR plasmid was cut with I-*Sce* I *in vitro*, and then co-injected either with Std-MO or with *lig4*-MO. HR repair analysis was carried out either by fluorescent observation (**A**) or by qPCR (**B**). **C** and **D:** SSA plasmid was co-injected either with Std-MO or with *lig4*-MO. SSA repair analysis was carried out either by fluorescent observation (**C**) or by qPCR (**D**).

development, since none of these studies used ionizing radiation or DSB reporter system to measure the accurate efficiency of HR and NHEJ in the early stages of embryogenesis, especially during the pre-blastocyst stage. To better understand the roles and regulation of DNA DSB repair pathways during development, it is necessary to set up reporter systems to analyze DNA DSB repair at the organismal level.

Two previous reports had successfully performed NHEJ, SSA and HR assays in *Xenopus*, *Drosophila*, and zebrafish embryos by utilizing antibiotic resistance genes (including the tetracycline, kanamycin and chloramphenicol resistance genes) as reporter genes (Hagmann et al., 1996, 1998). Their results showed that NHEJ was predominant in early embryogenesis. In their systems, repair events of different DNA DSB repair mechanisms were determined by a number of antibiotic resistance bacterial colonies, which were transformed with DNA extracted from the embryos injected with specific digested reporter construct. So their assay systems could not be directly visualized and the total amount of plasmid DNA injected was difficult to be normalized. Therefore, it might not be suitable to use their systems for the measurement of accurate efficiencies of DNA DSB repair pathways. Since common restriction endonuclease recognition sites were used to initiate DNA DSB in their systems, their designs were not suitable for generating DNA DSB *in vivo* as genomic DNA of injected embryos would be massively damaged. In this report, we combined the *EGFP* reporter gene and I-*Sce* I meganuclease to develop three visual-plus quantitative analysis systems for HR, SSA and NHEJ respectively in zebrafish embryos. In our systems, the efficiency of each repair mechanism could be easily visualized by EGFP expression and accurately measured by qPCR. As I-*Sce* I recognition sites were used in our systems, the DNA DSB could be initiated *in vivo*, allowing the use of the constructs to generate transgenic stabilized fish line.

Results from frequency analysis of each repair mechanism with our systems further confirmed that NHEJ is predominant during early embryogenesis in zebrafish, which supports the

findings of studies using somatic cell lines and *Xenopus*, *Drosophila* embryos. Strong fluorescence was observed at 7 hpf in the embryo injected with only 15 pg of the cut NHEJ, whereas weak fluorescence was detected in the embryo injected with up to 100 pg of the cut HR (Fig. 1B). Quantitative assay showed that the frequency of NHEJ (24.42%) (Fig. 2D) was much higher than the frequency of HR (1.89%) (Fig. 2C). DNA sequencing at the break site also revealed that about 80% of the repaired DSBs in the HR assay were carried out *via* the NHEJ pathway (Table 1).

To create HR and SSA constructs, one I-*Sce* I recognition site is normally inserted into the *EGFP* coding sequence to generate DSBs in cell lines. Most experiments have shown that the frequency of HR is less than 1% in the transfected cells analyzed by FACS assay. One possibility for the low frequency of HR in these analyses might be due to complementary overhangs generated by I-*Sce* I digestion, which can be re-ligated efficiently by NHEJ (Wilson et al., 1982). However, fluorescence cannot be visualized at the organism level if the repair frequency is too low. This might be the reason why we were unable to observe fluorescence from the embryos injected with the cut HR harboring only one I-*Sce* I site. To prove this presumption, we first used the large (Klenow) fragment of DNA polymerase I to remove the 3′ overhangs to form blunt ends followed by phosphatase treatment to remove 5′-phosphate. Fluorescence from the embryos injected with blunt ends of HR and SSA obviously increased, compared to controls with sticky ends (unpublished data). Our modified designs and the use of two opposite I-*Sce* I sites instead of one site worked efficiently. We reasoned that two opposite cleaved I-*Sce* I sites generated two partial complementary overhangs which enhance HR and SSA pathways by lowering the chances of NHEJ re-ligation repair. Our enhanced design should be applicable for other organisms.

Results from knockdown of *rad51*, *rad52* and *lig4* showed that their functions in these three DNA DSB repair pathways were conserved among species and loss of functions of these genes resulted in abnormal embryonic development. Our studies demonstrated that zebrafish provides an excellent system to investigate DNA DSB repair at the organismal level. In addition, the observation of HR in zebrafish embryos provides evidence that gene knock-in technique which relies on HR could be applied to this organism.

ACKNOWLEDGEMENTS

The work was supported by the National Natural Science Foundation of China (No. 30971677), the National Basic Research Program of China (973 Program) (No. 2012CB944500) and the Fundamental Research Funds for the Central Universities (No. 2011XZZX006).

SUPPLEMENTARY DATA

Fig. S1. Knockdown of *rad51* caused abnormal embryonic development in zebrafish.

Fig. S2. Influence of *rad52* knockdown on zebrafish embryonic development.

Fig. S3. Abnormal embryonic development of *lig4* morphants.

Supplementary data associated with this article can be found in the online version at http://dx.doi.org/10.1016/j.jgg.2012.07.009.

REFERENCES

Adams, B.R., Hawkins, A.J., Povirk, L.F., Valerie, K., 2010. ATM-independent, high-fidelity nonhomologous end joining predominates in human embryonic stem cells. Aging (Albany NY) 2, 582−596.

Akyuz, N., Boehden, G.S., Susse, S., Rimek, A., Preuss, U., Scheidtmann, K.H., Wiesmuller, L., 2002. DNA substrate dependence of p53-mediated regulation of double-strand break repair. Mol. Cell. Biol. 22, 6306−6317.

Certo, M.T., Ryu, B.Y., Annis, J.E., Garibov, M., Jarjour, J., Rawlings, D.J., Scharenberg, A.M., 2011. Tracking genome engineering outcome at individual DNA breakpoints. Nat. Methods 8, 671−676.

Chen, J., Ng, S.M., Chang, C., Zhang, Z., Bourdon, J.C., Lane, D.P., Peng, J., 2009. p53 isoform *Δ113p53* is a p53 target gene that antagonizes p53 apoptotic activity *via* BclxL activation in zebrafish. Genes Dev. 23, 278−290.

Ciccia, A., Elledge, S.J., 2010. The DNA damage response: making it safe to play with knives. Mol. Cell 40, 179−204.

Colleaux, L., D'Auriol, L., Galibert, F., Dujon, B., 1988. Recognition and cleavage site of the intron-encoded omega transposase. Proc. Natl. Acad. Sci. USA 85, 6022−6026.

Dudas, A., Chovanec, M., 2004. DNA double-strand break repair by homologous recombination. Mutat. Res. 566, 131−167.

Hagmann, M., Adlkofer, K., Pfeiffer, P., Bruggmann, R., Georgiev, O., Schaffner, D., Rungger, W., 1996. Dramatic changes in the ratio of homologous recombination to nonhomologous DNA-end joining in oocytes and early embryos of *Xenopus laevis*. Biol. Chem. Hoppe Seyler 377, 239−250.

Hagmann, M., Bruggmann, R., Xue, L., Georgiev, O., Schaffner, W., Rungger, D., Spaniol, P., Gerster, T., 1998. Homologous recombination and DNA-end joining reactions in zygotes and early embryos of zebrafish (*Danio rerio*) and *Drosophila melanogaster*. Biol. Chem. 379, 673−681.

Hakem, R., 2008. DNA-damage repair; the good, the bad, and the ugly. EMBO J. 27, 589−605.

Hiom, K., 2010. Coping with DNA double strand breaks. DNA Repair (Amst) 9, 1256−1263.

Ivanov, E.L., Sugawara, N., Fishman-Lobell, J., Haber, J.E., 1996. Genetic requirements for the single-strand annealing pathway of double-strand break repair in *Saccharomyces cerevisiae*. Genetics 142, 693−704.

Jasin, M., 1996. Genetic manipulation of genomes with rare-cutting endonucleases. Trends Genet. 12, 224−228.

Keimling, M., Wiesmuller, L., 2009. DNA double-strand break repair activities in mammary epithelial cells − influence of endogenous p53 variants. Carcinogenesis 30, 1260−1268.

Lieber, M.R., Ma, Y., Pannicke, U., Schwarz, K., 2003. Mechanism and regulation of human non-homologous DNA end-joining. Nat. Rev. Mol. Cell Biol. 4, 712−720.

Mills, K.D., Ferguson, D.O., Essers, J., Eckersdorff, M., Kanaar, R., Alt, F.W., 2004. Rad54 and DNA Ligase IV cooperate to maintain mammalian chromatid stability. Genes Dev. 18, 1283−1292.

Orii, K.E., Lee, Y., Kondo, N., McKinnon, P.J., 2006. Selective utilization of nonhomologous end-joining and homologous recombination DNA repair pathways during nervous system development. Proc. Natl. Acad. Sci. USA 103, 10017−10022.

Pierce, A.J., Johnson, R.D., Thompson, L.H., Jasin, M., 1999. XRCC3 promotes homology-directed repair of DNA damage in mammalian cells. Genes Dev. 13, 2633−2638.

Porter, G., Westmoreland, J., Priebe, S., Resnick, M.A., 1996. Homologous and homeologous intermolecular gene conversion are not differentially affected by mutations in the DNA damage or the mismatch repair genes

RAD1, RAD50, RAD51, RAD52, RAD54, PMS1 and *MSH2*. Genetics 143, 755−767.

Sung, P., Krejci, L., Van, K.S., Sehorn, M.G., 2003. Rad51 recombinase and recombination mediators. J. Biol. Chem. 278, 42729−42732.

Thoms, K.M., Kuschal, C., Emmert, S., 2007. Lessons learned from DNA repair defective syndromes. Exp. Dermatol. 16, 532−544.

Tichy, E.D., Pillai, R., Deng, L., Liang, L., Tischfield, J., Schwemberger, S.J., Babcock, G.F., Stambrook, P.J., 2010. Mouse embryonic stem cells, but not somatic cells, predominantly use homologous recombination to repair double-strand DNA breaks. Stem Cells Dev. 19, 1699−1711.

Tichy, E.D., Stambrook, P.J., 2008. DNA repair in murine embryonic stem cells and differentiated cells. Exp. Cell Res. 314, 1929−1936.

Weinstock, D.M., Nakanishi, K., Helgadottir, H.R., Jasin, M., 2006. Assaying double-strand break repair pathway choice in mammalian cells using a targeted endonuclease or the RAG recombinase. Methods Enzymol. 409, 524−540.

Weterings, E., Chen, D.J., 2008. The endless tale of non-homologous end-joining. Cell Res. 18, 114−124.

Wilson, J.H., Berget, P.B., Pipas, J.M., 1982. Somatic cells efficiently join unrelated DNA segments end-to-end. Mol. Cell. Biol. 2, 1258−1269.